JOURNAL OF AGRICULTURAL AND FOOD CHEMISTRY

Spermidine and Flavonoid Conjugates from Peanut (*Arachis hypogaea*) Flowers

VICTOR S. SOBOLEV,*,† ARLENE A. SY,‡ AND JAMES B. GLOER‡

National Peanut Research Laboratory, Agricultural Research Service, U.S. Department of Agriculture, Dawson, Georgia 39842, and Department of Chemistry, University of Iowa, Iowa City, Iowa 52242

A new spermidine triamide derivative has been isolated from peanut flowers and identified as N^1-acetyl-N^5,N^{10}-di-*p*-(*EE*)-coumaroylspermidine on the basis of detailed analysis of NMR, MS, and UV data. Two other spermidine conjugates, N^1,N^5,N^{10}-tri-*p*-(*EEE*)-coumaroylspermidine and di-*p*-(*EE*)-coumaroylspermidine, as well as four flavonoid conjugates (quercetin-3-glucoside, quercetin-3-glucuronide, isorhamnetin-3-glucoside, and isorhamnetin-3-glucuronide) that have been previously reported in organs of other plants, have been found in this study in peanut (*Arachis hypogaea* L.), a representative of the Leguminosae family, for the first time. The dynamics of photoisomerization in the spermidine conjugates have been investigated.

KEYWORDS: Peanuts; *Arachis hypogaea*; groundnuts; *p*-coumaric acid; coumaroylspermidine; dicoumaroylacetylspermidine; tricoumaroylspermidine; quercetin glucoside; quercetin glucuronide; isorhamnetin glucoside; isorhamnetin glucuronide; photochemical isomerization; structure elucidation; NMR; HPLC-MS

INTRODUCTION

Peanuts are an economically important crop. Sound seed yield depends heavily on high resistance to pests and uncompromised plant fertility. Peanuts are self-pollinating plants with unusual inflorescence and infructescence. The first flowers appear 4−6 weeks after planting. Flowering continues for 6 or more weeks. There may be several flowers in an inflorescence on the plant, but only one opens on a given morning, and there is an interval from one to several days between the openings of successive flowers (*1*). The flower opens at sunrise, and pollen shedding takes place. Fertilization occurs 8−9 h after pollination (*2*). Then, the flower fades, and the ovary elongates to become the peg, which drives into the soil where it matures into a pod with seeds. Peanut flowers have been considered resistant to pests (*3, 4*) with one exception being *Heliothis* spp. caterpillars (*5*). Compounds that may be responsible for such resistance have not been investigated.

Flavonoids are pigments that are crucial for plants (*6, 7*). One of their major functions in plants is protection, as they kill or inhibit the growth or reproduction of several pathogenic bacterial, fungal, and viral strains as well as protozoans. However, the toxicity of flavonoids to herbivorous animals is low (*6, 8*). Flavonoids are found in different organs of plants in free or bound forms (*6, 7*). The flavonoid content is often used by scientists for taxonomic purposes (*8*).

Hydroxycinnamic acid amides (HCAA) are a widely distributed group of plant secondary metabolites that are concentrated in the floral parts of plants (*9–18*). Several HCAA have been isolated and identified (*12–17, 19*). Some fundamental functions have been attributed to these amides, including protection against fungi, bacteria, viruses, and insects (*20–28*), influence on growth, cell multiplication, floral induction, flower formation, sexual differentiation, tuberization, cell division, and cytomorphogenesis (*16, 20, 25, 29–32*). It has been found that HCAA accumulation in strawberry is associated with plant irradiation with light (*33*). Hydroxycinnamic acid−spermidine conjugates have proven useful for chemotaxonomic classification in several plant families (*12*). In addition to diverse functions in plants, three of the HCAAs, particularly N^1,N^5,N^{10}-tri-*p*-coumaroylspermidine, have been reported to appreciably inhibit HIV-1 protease that is essential for the life cycle of HIV (*34*). The latter compound also demonstrated a high activity against *Helicobacter pylori*, a major etiological agent in gastroduodenal disorders (*35*). The goal of this research was to investigate the presence of major phytochemicals in different organs of the peanut flower that may be responsible for peanut fertility and protection against pests.

EXPERIMENTAL PROCEDURES

Reagents, Materials, and Basic Apparatus. High-performance liquid chromatography (HPLC)-grade solvents used in the preparation of mobile phases, sample extraction, separations on silica gel, and isomerization were obtained from Fisher (Suwanee, GA). Silica gel for thin-layer chromatography (TLC; silica gel 60H) and for column chromatography (silica gel 60, 0.063–0.200 mm) were purchased from EM Science (Gibbstown, NJ). Na_2SO_4 was purchased from J. T. Baker.

* To whom correspondence should be addressed. Tel: 229-995-7446. Fax: 229-995-7416. E-mail: victor.vsobolev@ars.usda.gov.
† U.S. Department of Agriculture.
‡ University of Iowa.

10.1021/jf703652a CCC: $40.75
Published on Web 04/16/2008

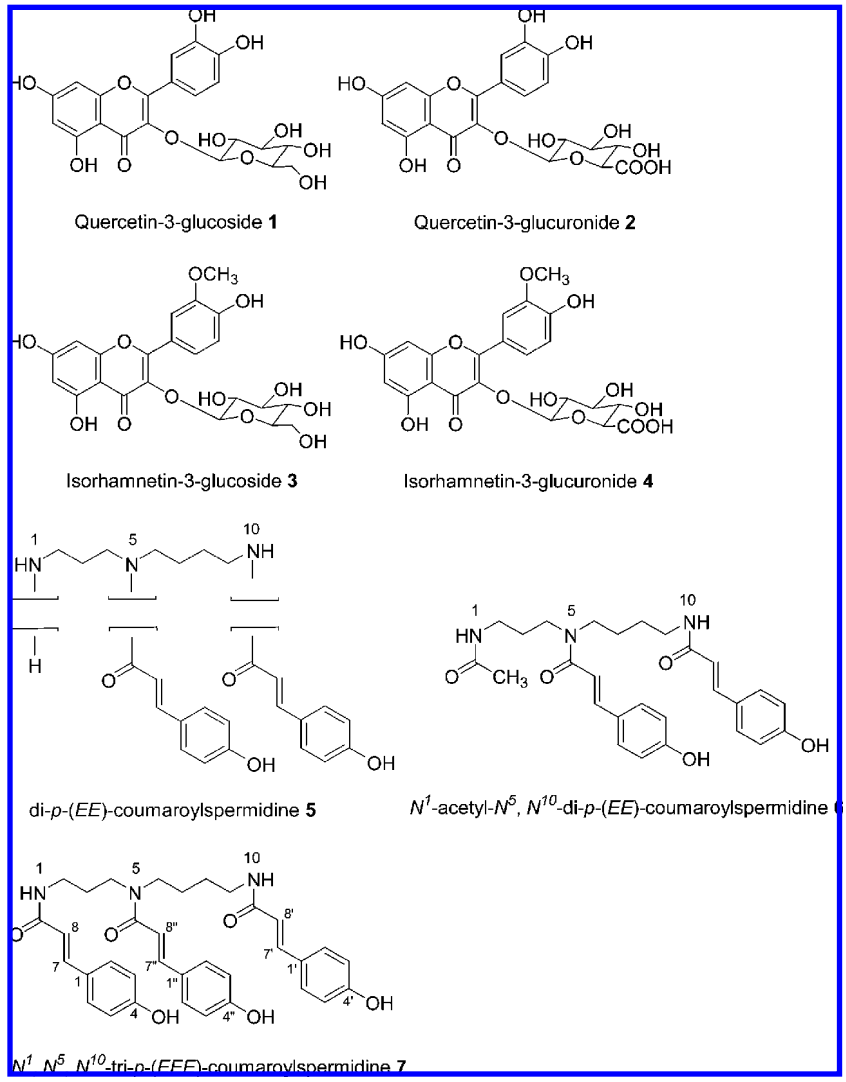

Figure 1. Structures of peanut flavonoid and spermidine conjugates.

A high-speed blender with a 1 L glass jar (13000 rpm; General Electric), a rotary evaporator (bath temperature, 40°), and an ultrasonic bath were used in the research. A 2 L Kimax Büchner type filtering funnel (i.d. 125 mm) with 10–15 μm fritted disk was used as a column for preparative chromatography.

Reference Compound. *p*-Coumaric acid was purchased from Aldrich. ESI-MS/MS (MS^2) and UV data were obtained for the above commercial compound to serve as a comparison standard for identification of *p*-coumaric acid extracted from peanut flowers. ESIMS analysis of this phenolic acid gave an $[M - H]^-$ ion at *m/z* 163 and UV maxima at 293 sh, 300 sh, and 308 nm.

Plant Material. Plant materials included five lines from Runner market type and six Virginia market type; Runner market types: Tifrunner, G02C, C724-19-15, AT29-1112, and AT3-1114; Virginia market types: VC-2, AT3081 R, Gregory, AT3085RO, and experimental breeding lines termed in this publication A and B. Four plants in each 28″ L × 12″ W × 10″ D pot with local commercial pot soil were grown in a temperature-, illumination-, and humidity-controlled green house. The plants received normal management practices. Peanut flowers, with about 10 mm long hypanthium, were collected each morning (from 7 to 9 a.m.) from August 1, 2007 to August 21, 2007. Whole peanut flowers were frozen at −40 °C immediately after their collection to stop possible enzymatic reactions; frozen samples were stored at this temperature before analysis.

Extraction and Purification. A 20 g sample of whole peanut flowers was extracted with 100 mL of MeOH in a high-speed blender for 2 min. Filtered aliquots of the extract were used for direct determination of target constituents by HPLC.

For preparative isolation of conjugates, 800 g of peanut flowers combined from 11 lines was extracted portionwise (100 g each) with 2.4 L of MeOH (300 mL for each portion) in a high-speed blender for 2 min. The combined mixture was filtered through a glass fiber filter in a Büchner type funnel under reduced pressure. The solid residue was resuspended in 2 L of MeOH, and the extraction procedure was repeated twice as described above. The combined extract solutions were filtered through a filter paper and defatted twice with 0.5 L of *n*-hexane. The MeOH layer was evaporated nearly to dryness with 100 g of silica gel for column chromatography using a rotary evaporator. To remove excess water from the silica gel, an appropriate amount of acetonitrile was added close to the end of evaporation, and the mass was evaporated to dryness. The silica gel appeared as free-flowing powder. For isolation of target compounds, a 2 L filtering funnel packed with 330 g of silica gel for TLC (suspended in $CHCl_3$) was used as a column for preparative chromatography (column #1). Dry silica gel with the flower extract adsorbed was resuspended in $CHCl_3$ and applied to the column. The column was subsequently eluted with 1 L of $CHCl_3$, 2 L of EtOAc, 1.5 L of EtOAc−acetone (5:1, v/v), 2 L of EtOAc−acetone (1:1, v/v), 1.5 L of acetone, and 1.5 L of MeOH. Twenty-five fractions were collected from the column and analyzed by HPLC. Fractions containing target flavonoid conjugates and spermidine conjugates (**Figure 1**) were separately combined, evaporated to dryness with a rotary evaporator, and subjected to further purification.

Purification of Flavonoid Conjugates. Combined flavonoid fractions were dissolved in MeOH, filtered, and subjected to a final purification on a 100 mm × 19 mm i.d., 5 μm, XTerra Prep RP_{18} OBD preparative HPLC column (Waters) using gradient elution profile. The mobile phase

(termed mobile phase #1 for further simplicity) consisted of H_2O (A), CH_3CN (B), and 2% HCOOH in H_2O (C). The solvents were mixed in the following gradient: initial conditions, 65% A/30% B/5% C hold for 1 min, increase linearly to 0% A/95% B/5% C in 10 min, hold isocratic for 3 min, decrease to initial conditions in 0.01 min. The flow rate was 7.5 mL/min. Combined fractions containing flavonoid conjugates were evaporated with a rotary evaporator to a point where almost all of the MeOH was removed. The remaining aqueous mixture containing the target compounds was extracted four times with EtOAc (H_2O−EtOAc ratio 1:3, v/v). The combined EtOAc layers were evaporated nearly to dryness with a rotary evaporator. The residue was transferred into a 15 mL vial with MeOH and evaporated to dryness under a stream of N_2.

Purification of Spermidine Conjugates. Combined fractions containing the spermidines were resuspended in $CHCl_3$, sonicated in an ultrasonic bath for 1 min, and applied to silica gel column #2 (350 × 40 mm). The column was subsequently eluted with $CHCl_3$ (300 mL), EtOAc (400 mL), EtOAc−acetone (300 mL + 75 mL), acetone (400 mL), $CHCl_3$−MeOH (300 mL + 75 mL), and MeOH (400 mL). Fourteen fractions were collected. Tricoumaroylspermidine was mainly eluted with the EtOAc, EtOAc−acetone, and acetone-eluting solvents. Dicoumaroylacetylspermidine was mainly eluted with the $CHCl_3$−MeOH mixture. Fractions containing tricoumaroylspermidine and dicoumaroylacetylspermidine were redissolved in EtOAc−acetone (2:1, v/v) and separately applied to two Al_2O_3 columns (80 mm × 27 mm each; columns #3 and #4). The columns were subsequently eluted with EtOAc−acetone (50 mL + 50 mL), acetone (250 mL), MeOH (100 mL), and MeOH−H_2O−HCOOH (196 mL + 3.5 mL + 0.5 mL). The spermidines were eluted from both columns with the last solvent mixture. Fractions containing spermidine conjugates were evaporated to dryness. The fraction containing tricoumaroylspermidine was redissolved in MeOH, filtered, and subjected to a final purification on preparative HPLC column under isocratic conditions. The mobile phase (termed mobile phase #3) consisted of 70% H_2O (A), 28% CH_3CN (B), and 2% of 2% HCOOH in H_2O (C). The flow rate was 9.0 mL/min. Fractions from the HPLC column containing tricoumaroylspermidine were evaporated with a rotary evaporator to a point where almost all CH_3CN was removed. The remaining aqueous mixture containing the target compound was extracted four times with EtOAc (H_2O:EtOAc ratio 1:4, v/v). The combined EtOAc layers were evaporated nearly to dryness with a rotary evaporator. The residue was resuspended in MeOH, transferred into a 4 mL vial, and evaporated to dryness under a stream of N_2.

Fractions from aluminum oxide column #4 containing dicoumaroylacetylspermidine were combined and evaporated with a rotary evaporator to a point where almost all MeOH was removed. The remaining aqueous mixture containing the target compound was extracted four times with EtOAc (H_2O−EtOAc ratio 1:3, v/v). The combined EtOAc layers were evaporated nearly to dryness with a rotary evaporator. The residue was transferred into a 15 mL vial with MeOH and evaporated to dryness with in a stream of N_2. For additional purification of the compound, the residue was dissolved in EtOAc−acetone (2:1, v/v) and applied to silica gel column #5 (120 mm × 30 mm). The column was subsequently eluted with $CHCl_3$−MeOH mixtures of increasing polarity (250 + 5, 250 + 10, 250 + 15, 250 + 25, 250 + 40, and 250 + 50 mL). Fractions containing the target compound were combined, evaporated with a rotary evaporator to dryness, redissolved in MeOH, and subjected to final purification on a preparative HPLC column under isocratic conditions. The mobile phase (termed mobile phase #2) consisted of 74% H_2O (A), 24% CH_3CN (B), and 2% of 2% HCOOH in H_2O (C). The flow rate was 8.5 mL/min. Isolation of the compound was performed as described above for tricoumaroylspermidine.

For extraction from peanut flowers, whole flowers as well as different parts of the flower were used. The flowers were separated into four parts: standard, wings, keel, and hypanthium (**Figure 2**). Separated parts were ground in an agate mortar with an equal amount (w/w) of Celite 545. The mixtures were extracted with a triple amount of MeOH (w/v) for 30 min with periodic (every 5 min) vortexing for 30 s. Each extract was filtered through a glass fiber filter. From 5 to 30 μL of each filtrate was analyzed by HPLC.

Figure 2. Peanut flower. Key: 1, standard; 2, one of two symmetrical wings (one of the wings is removed for a better observation of the keel); 3, keel (two fused petals that enclose pistil and stamens); and 4, hypanthium.

HPLC-DAD Analyses. Analyses were performed using an HPLC system equipped with a model LC-10ATvp pump (Shimadzu), a model SPD-M10Avp DAD (with Shimadzu Client/Server software, version 7.3) covering the 200–600 nm range, and a model 717 plus autosampler (Waters). The separations of whole flower extracts and purified flavonoid conjugates were performed on a 150 mm × 4.6 mm i.d., 3.5 μm, XTerra MS C18 analytical column (Waters). H_2O (A), MeOH (B), and 2% of HCOOH in H_2O (C) were used in the following gradient: initial conditions, 68% A/30% B/2% C, increase linearly to 0% A/98% B/2% C in 22 min, hold isocratic for 5 min, decrease to initial conditions in 0.01 min. For separations of spermidine conjugates and their photoisomerization products, an isocratic mobile phase composed of 74% of (A), 2% of (C), and 24% of (D) was used. The flow rate in both cases was 1.0 mL/min. The column was maintained at 40 °C in a model 105 column heater (Timberline Instruments; Boulder, CO). The eluate from the DAD was split with a T-unit (Upchurch Scientific; Oak Harbor, WA) for optimal MS performance. The flow rate through the ESI probe was set at 0.35 mL/min.

Photoisomerization of Peanut Spermidine Conjugates 6 and 7. For analytical purposes, 0.5−20 mL of ca. 0.001% solution of the conjugates in MeOH or mobile phases #2 and #3 was placed in polypropylene or borosilicate vials and irradiated in direct sunlight from 10 s to 3 h depending on the objective of the experiments. For preparative purposes, combined eluates (up to 250 mL) from the preparative HPLC column were placed in Pyrex flasks and irradiated in sunlight for 20 min. The experiments were performed at latitude 31.75° N in the middle of November from 11 a.m. to 1 p.m. with clear sky; the intensity of the sunlight was not measured. Separation of the photoisomers was accomplished as described above for the natural spermidine conjugates using the same preparative HPLC column and mobile phase #2. Alternatively, for analytical purposes, a MeOH solution of spermidine conjugates was placed into 4 mL borosilicate vials equipped with lids with Teflon septa. The vials were placed in a horizontal position on a sheet of aluminum foil inside a UV viewing cabinet equipped with 4 × 15 W fluorescent lamps and irradiated from a distance of 15 cm from 1 to 60 min. Photoisomerization at different temperatures (−95, 30, and 100 °C) was performed in a sealed ampule, which was brought to a desired temperature under dim light and then exposed to sunlight for 15 min. To maintain temperature at 100 °C, the ampule was placed in a beaker with boiling water. For a low-temperature experiment, the ampule was placed in a beaker filled with MeOH, covered with a glass plate, and positioned in a Dewar flask with liquid N_2 so that most of MeOH became frozen; the temperature was monitored with a thermometer.

Data Analysis. Data were analyzed by the analysis of variance method using SAS, 2000 (SAS Institute, Inc., Version 8, Cary, NC). Comparisons of the various means were performed by least significant difference (LSD) test at $p = 0.05$. The Pearson product−moment correlation coefficient was calculated using SigmaStat (version 3.1, SYSTAT Software, Inc., Point Richmond, CA). Comparison of means of two groups of data was performed using the t test. The Mann–Whitney rank sum test was applied when the normality test failed ($p < 0.05$).

Spectroscopic Measurements. UV measurements were performed with a Varian Cary 100 Bio UV–vis spectrophotometer. ^{1}H NMR, ^{13}C NMR, and homonuclear decoupling experiments were performed on a

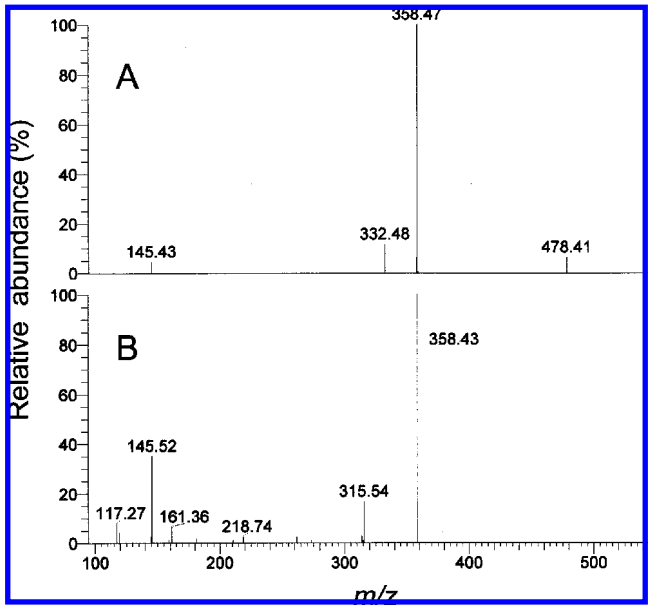

Figure 3. Negative ion ESI-MS spectra of N^1-acetyl-N^5,N^{10}-di-*p*-(*EE*)-coumaroylspermidine (**6**). (**A**) *m*/*z* 478 at 38; (**B**) *m*/*z* 478 at 38 → 358 at 45.

Bruker DRX-400 or a Bruker AC-300. HMBC and HMQC experiments were performed on a Bruker AMX-600 spectrometer. Chemical shift values were referenced to the solvent signals for CD_3OD (δ_H 3.31/δ_C 49.1) or DMSO-d_6 (δ_H 2.50/δ_C 39.5). HRESIMS and EIMS data were recorded on a Micromass Autospec instrument. ESI-MS/MS^2 data were obtained on a Finnigan LCQ Advantage MAX ion trap mass spectrometer equipped with an ESI interface and operated with Xcalibur version 1.4 software (Thermo Electron Corp., San Jose, CA). The data were acquired in the full-scan mode from *m*/*z* 100 to 2000. The heated capillary temperature was 240 °C, the sheath gas flow was 45 units, the capillary voltage was 10 V in positive mode and −4 V in negative, and the source voltage was 5.0 kV. In MS^2 analyses, the $[M + H]^+$ and $[M - H]^-$ ions observed for each chromatographic peak in full-scan analyses were isolated and subjected to source collision-induced dissociation (CID) using He buffer gas. In all CID analyses, the isolation width, relative fragmentation energy, relative activation Q, and activation time were *m*/*z* = 2.6, 20–45%, 0.25, and 30 ms, respectively. Concentrations of compound of interest were determined by reference to peak areas of corresponding pure compounds. The results of MS^2 experiments are represented throughout the text as follows: *m*/*z* aaa at bb → aaa, ccc, ddd, where aaa is parent ion, bb is normalized collision energy (%), and ccc and ddd are fragment ions.

UV spectra in mobile phase #1 for flavonoid conjugates **1**, **2**, **3**, and **4** are given in the Supporting Information section. The UV spectra as well as MS and MS^2 data were nearly identical to those in the literature (*36*–*38*), with a characteristic loss of 162 Da from the negatively charged pseudomolecular ions ($[M - H]^-$) of glucosides **1** and **3** (*m*/*z* 463 and 477, respectively) and a loss of 176 Da from the pseudomolecular ions of glucuronides **2** and **4** (*m*/*z* 477 and 491, respectively).

Di-p-(EE)-coumaroylspermidine ***5.*** Negative ESI-MS^2 *m*/*z* 436 at 35: 436 ($[M - H]^-$; rel int 65), 316 ($[M - H]^- - OH{-}C_6H_4{-}CH{=}CH$; 100), 290 (1.2), 145 ($[M - H]^-$ − spermidine; 10). Positive ESI-MS^2 *m*/*z* 438 at 35: 438 ($[M + H]^+$; 100), 422 (4.0), 292 (17), 274 (2.3), 204 (17), 147 (4.0). The MS data agree with those published in the literature (*10*).

N^1*-Acetyl-*N^5,N^{10}*-di-p-(EE)-coumaroylspermidine* ***6.*** White solid from CH_3CN and EtOAc; clear, very slightly greenish glass from MeOH. UV (mobile phase #2) λ_{max} (nm): 222, 292sh, 306. Negative ESI-MS (**Figure 3**): *m*/*z* 478 at 38: 478 ($[M - H]^-$; 7.1), 358 ($[M - H]^- - HO{-}C_6H_4{-}CH{=}CH$; 100), 332 ($[M - H]^-$ − *p*-coumaroyl unit; 12), 145 ($[M - H]^-$ − spermidine; 4.9). Negative ESI-MS^3 (**Figure 3**) *m*/*z* 478 at 38 → 358 at 45: *m*/*z* 358 ($[M - H]^- - HO{-}C_6H_4{-}CH{=}CH$; 100), 315 ($[M - H]^- - HO{-}C_6H_4{-}CH{=}CH$ − acetyl; 17), 145.5 ($[M - H]^-$ − spermidine; 35). Positive ESI-MS^2 *m*/*z* 480 at 35: 462 ($[M + H - H_2O]^+$; 2.2), 420 (11), 410 (3.3), 360 (4.0), 334 (89), 316 (100), 303 (46), 171 (8.6). EIMS (70 eV): The molecular ion was not observed, but major fragment ions of potential significance were observed at *m*/*z* 333 (9), 293 (7), 265 (8), 247 (12), 186 (8), 181 (8), 169 (13), 147 (100), 129 (39), 119 (25), 100 (30), 84 (15), 70 (37), 69 (37). HREIMS data for selected key fragments: obsd *m*/*z* 333.2017, calcd for $C_{18}H_{27}N_3O_3$, 333.2052; obsd *m*/*z* 247.1423, calcd for $C_{14}H_{19}N_2O_2$, 247.1447; obsd *m*/*z* 169.1350, calcd for $C_9H_{17}N_2O$, 169.1341; obsd *m*/*z* 147.0448, calcd for $C_9H_7O_2$, 147.0446; obsd *m*/*z* 129.1028, calcd for $C_6H_{13}N_2O$, 129.1028. ^{1}H NMR at room temperature (400 MHz, DMSO-d_6): *p*-coumaroyl systems: δ 7.80–7.98 (m, NH-1 and NH-10), 7.26–7.51 (m, H-2, H-2′, H-6, H-6′, H-7 and H-7′), 6.70–6.85 (m, H-3, H-3′, H-5, H-5′, H-8′), 6.32–6.38 (m, H-8). Spermidine system: 3.00–3.50 (m, H_2-2, H_2-4, H_2-6, and H_2-9; partially obscured by water peak), 1.80 (br s, acetyl CH_3), 1.40–1.70 (m, H_2-3, H_2-7, and H_2-8). ^{1}H NMR at 55 °C (400 MHz, DMSO-d_6): *p*-coumaroyl systems: δ 7.27–7.51 (m, H-2, H-2′, H-6, H-6′, H-7 and H-7′), 6.78 (d, J = 16, H-8 or H-8′), 6.70–6.76 (m, H-3, H-3′, H-5, H-5′), 6.35 (d, J = 16, H-8 or H-8′). Spermidine system: δ 7.80 (br s, NH-1 and NH-10), 3.00–3.50 (m, H_2-2, H_2-4, H_2-6, and H_2-9; partially obscured by water peak), 1.80 (s, acetyl CH_3) 1.40–1.70 (m, H_2-3, H_2-7, and H_2-8).

N^1*-Acetyl-*N^5,N^{10}*-di-p-(ZZ)-coumaroylspermidine (Peak f,* ***Figure 4****).* White solid from EtOAc. UV (mobile phase #2) λ_{max} (nm) 268. MS data were nearly identical to those of the *EE* isomer **6**.

N^1*-Acetyl-*N^5,N^{10}*-di-p-(ZE)-coumaroylspermidine (Peak g,* ***Figure 4****).* White solid from EtOAc. UV (mobile phase #2) λ_{max} (nm) 217sh, 279sh, 285, 301sh. MS data were nearly identical to those of the *EE* isomer **6**.

N^1*-Acetyl-*N^5,N^{10}*-di-p-(EZ)-coumaroylspermidine (Peak h,* ***Figure 4****).* White solid from EtOAc. UV (mobile phase #2) λ_{max} (nm) 225, 292, 305sh. MS data were nearly identical to those of the *EE* isomer **6**.

N^1,N^5,N^{10}*-Tri-p-(EEE)-coumaroylspermidine* ***7.*** UV (mobile phase #3) λ_{max} (nm) 223, 292sh, 295, 304. HRESIMS *m*/*z* 584.2769 $[M + H]^+$, calcd for $C_{34}H_{37}N_3O_6$, 583.2684. Negative ESI-MS^2 *m*/*z* 582 at 35: 582 ($[M - H]^-$; 9.4), 462 ($[M - H]^- - OH{-}C_6H_4{-}CH{=}CH$; 100), 436 ($[M - H]^-$ − *p*-coumaroyl unit; 8.4), 342 ($[M - H]^- - OH{-}C_6H_4{-}CH{=}CH - OH{-}C_6H_4{-}CH{=}CH$; 3.2). Positive ESI-$MS^2$ *m*/*z* 584 at 35: 566 ($[M + H - H_2O]^+$; 2.1), 464 (5.6), 438 (70), 420 (100), 275 (1.2), 204 (0.5). ^{1}H NMR (room temperature, 400 MHz, CD_3OD): *p*-coumaroyl systems: δ 7.49–7.55 (m, H-7 and H-7′), 7.33–7.48 (m, H-2, H-2′, H-2″, H-6, H-6′, H-6″ and H-7″), 6.85 (m, H-8″), 6.70–6.83 (m, H-3, H-3′, H-3″, H-5, H-5′ and H-5″), 6.34–6.43 (m, H-8 and H-8′). Spermidine system: δ 3.32–3.60 (m, H_2-2, H_2-4, H_2-6, and H_2-9), 1.54–1.96 (m, H_2-3, H_2-7, and H_2-8). ^{1}H NMR (room temperature, 400 MHz, DMSO-d_6): *p*-coumaroyl systems: δ 7.27–7.54 (m, H-2, H-2′, H-2″, H-6, H-6′, H-6″, H-7, H-7′ and H-7″), 6.85 (m, H-8″), 6.67–6.77 (m, H-3, H-3′, H-3″, H-5, H-5′ and H-5″), 6.33–6.43 (m, H-8 and H-8′). Spermidine system: δ 7.94–8.10 (br m, NH-1 and NH-10), 3.12–3.50 (m, H_2-2, H_2-4, H_2-6, H_2-9), 1.40–1.80 (m, H_2-3, H_2-7, H_2-8). ^{1}H NMR at 95 °C (400 MHz, DMSO-d_6): *p*-coumaroyl systems: δ 7.28–7.46 (m, H-2, H-2′, H-2″, H-6, H-6′, H-6″, H-7, H-7′ and H-7″), 6.80 (d, J = 16, H-8″), 6.73–6.78 (m, H-3, H-3′, H-3″, H-5, H-5′ and H-5″), 6.37 (d, J = 16, H-8 or H-8′), 6.38 (d, J = 16, H-8 or H-8′). Spermidine system: δ 7.56–7.68 (br m, NH-1 and NH-10), 3.12–3.50 (m, H_2-2, H_2-4, H_2-6, H_2-9), 1.40–1.80 (m, H_2-3, H_2-7, H_2-8). The MS and UV data agree with those published in the literature (*10, 12, 28*).

The UV spectra of both **6** and **7** did not change in acidic (pH 4.0), neutral, or basic (pH 8.5) solutions. Neither of compounds steam distill. As expected, irradiation of **6** and **7** with green light (532 nm) from a 5 mW laser pointer for 40 min did not cause any change in the compounds, which indicates that green light illumination may be used during the isolation of the compounds.

N^1,N^5,N^{10}*-Tri-p-(ZZZ)-coumaroylspermidine (Peak a,* ***Figure 4****).* UV (mobile phase #3) λ_{max} (nm) 268. MS data were nearly identical to those of the *EEE* isomer **7**. ^{1}H NMR (400 MHz, CD_3OD): *p*-coumaroyl systems: δ 7.34–7.42 (m, H-2′ and H-6′), 7.18–7.23 (m, H-2″ and H-6″), 6.69–6.75 (m, H-3′, H-3″, H-5′ and H-5″), 6.50–6.65 (6 d, each with J = 13, H-7, H-7′ and H-7″) 5.75–5.92 (six doublets, each with J =

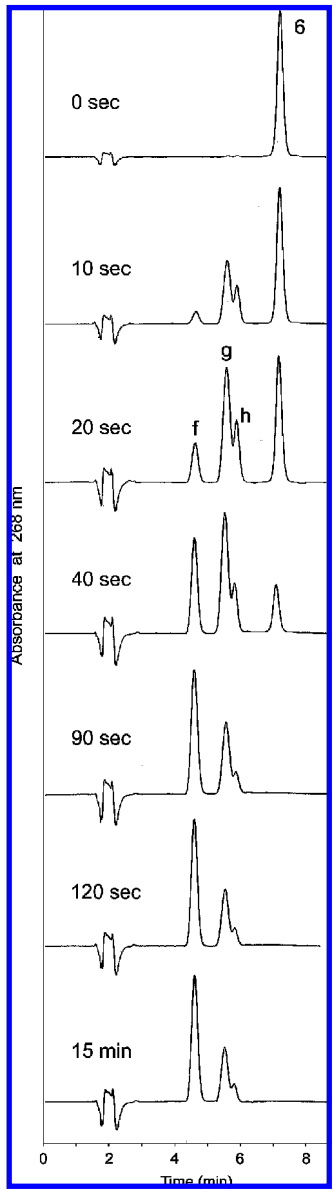

Figure 4. Dynamics of N^1-acetyl-N^5,N^{10}-di-*p*-(*EE*)-coumaroylspermidine **6** photoisomerization. Peaks: f, N^1-acetyl-N^5,N^{10}-di-*p*-(*EE*)-coumaroylspermidine; g and h, (*ZE*)- and (*EZ*)-di-*p*-coumaroylacetylspermidine isomers. Chromatograms were normalized by the highest peak.

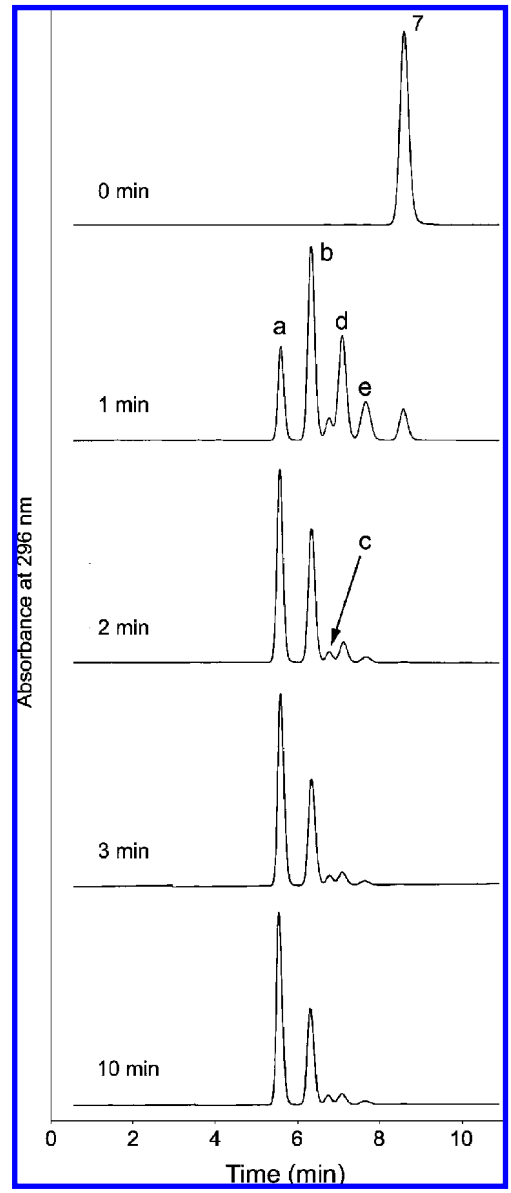

Figure 5. Dynamics of N^1,N^5,N^{10}-tri-*p*-(*EEE*)-coumaroylspermidine **7** photoisomerization. Peaks: a, N^1,N^5,N^{10}-tri-*p*-(*ZZZ*)-coumaroylspermidine; b, mixture of *ZZE* isomers of N^1,N^5,N^{10}-tri-*p*-coumaroylspermidine; c and d, mixture of *ZZE/EEZ* isomers; and e, mixture of *EEZ* isomers. Chromatograms were normalized by the highest peak.

13, H-8, H-8′, and H-8″ signals for both conformers). Spermidine system: 3.10–3.40 (m, H_2-2, H_2-4, H_2-6, H_2-9), 1.30–1.80 (m, H_2-3, H_2-7, H_2-8).

*Mixture of ZZE Isomers of N^1,N^5,N^{10}-Tri-p-coumaroylspermidine (Peak b, **Figure 4**).* UV (mobile phase #3) λ_{max} (nm) 279, 302sh. MS data were nearly identical to those of the *EEE* isomer **7**.

RESULTS AND DISCUSSION

Structure Elucidation. Three major peaks (1, 2, and 7; **Figure 6**) were detected in the flower extracts. Two of the peaks (1 and 2) were suggested to be flavonoid conjugates based on their characteristic absorption spectra (shown in the Supporting Information) and mass spectra. Inspection of the ^{1}H and ^{13}C NMR spectra for compounds **1** and **2** suggested that both compounds are flavonoid glycosides. In each instance, analysis of the data revealed the presence of a 1,3,5-trioxygenated 1,2,3,5-tetrasubstituted benzene ring and a 1,2-dioxygenated 1,2,4-trisubstituted benzene ring, as well as a six-carbon monosaccharide unit and three other sp^2 carbons, indicating the presence of a monoglycosylated quercetin analogue. The signals for the monosaccharide unit in compound **1** corresponded to those of a glucuronic acid unit, while those of compound **2** were consistent with the presence of a glucose moiety. ^{1}H NMR *J* values enabled assignment of a β-linkage in both cases. For both compounds, the signal for the anomeric proton showed an HMBC correlation to C-3 of the γ-pyrone ring, locating the monosaccharide unit at the 3-position of the flavonoid. Detailed analysis of the HMBC data was fully consistent with identification of these compounds as quercetin-3-glucoside and quercetin-3-glucuronide (**1** and **2**; **Figure 1**).

Compounds **3** and **4** were identified as isorhamnetin-3-glucoside and isorhamnetin-3-glucuronide, respectively, on the basis of MS and UV data. The compounds were not obtained in quantities conducive to independent structure determination by NMR analysis, so the positions of the glucosyl and glucuronyl moieties were not unambiguously confirmed. However, structures **3** and **4** are considered most likely since the

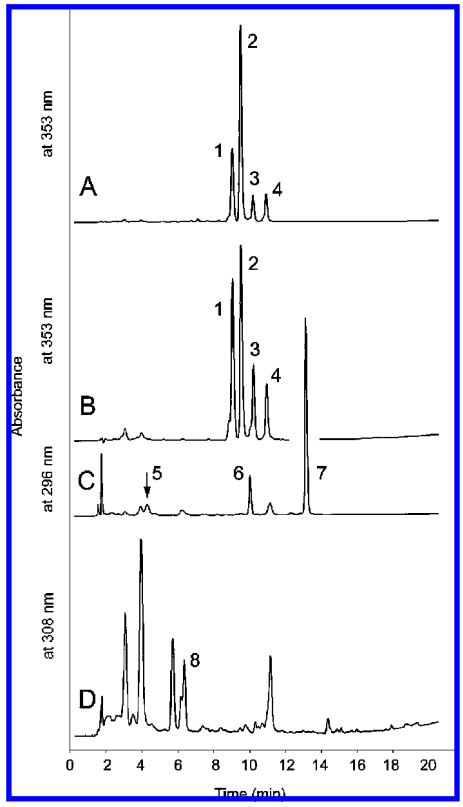

Figure 6. Flavonoid and spermidine conjugate contents in different parts of the peanut flower. (**A**) Standard, (**B**) wings, (**C**) keel, and (**D**) hypanthium. Key: 1, quercetin-3- glucoside **1**; 2, quercetin-3-glucuronide **2**; 3, isorhamnetin-3-glucoside **3**; 4, isorhamnetin-3-glucuronide **4**; 5, di-*p*-(*EE*)-coumaroylspermidine **5**; 6, N^1-acetyl-N^5,N^{10}-di-*p*-(*EE*)-coumaroylspermidine **6**; 7, N^1,N^5,N^{10}-tri-*p*-(*EEE*)-coumaroylspermidine **7**; and 8, *p*-(*E*)-coumaric acid. Chromatograms were normalized by the highest peak.

major compounds **1** and **2** bear 3-glucosyl and 3-glucuronyl units, respectively (**Figure 1**). In addition, MS and UV data for **3** and **4** were virtually identical to those published in the literature (*36–38*). Compounds **1** and **2** gave $[M - H]^-$ ions at *m/z* 463 and *m/z* 477, respectively. Upon MS^2 analysis, each produced a major fragment ion at *m/z* 301 ($[M - H]^-$ − 162 Da in **1** and $[M - H]^-$ − 176 Da in **2**, corresponding to loss of the glucose and glucuronide units, respectively). Compounds **3** and **4** afforded $[M - H]^-$ ions at *m/z* 477 and *m/z* 491, respectively, both of which fragmented by MS^2 to afford a major ion at *m/z* 315 ($[M - H]^-$ − 162 Da in **3** and $[M - H]^-$ − 176 Da in **4**, again corresponding to loss of the glucose and glucuronide units, respectively).

The UV spectrum of the third major peak (7) resembled those typical of *p*-hydroxycinnamic acids, but the compound could not be clearly identified based only on its UV and MS data. A database search for the accurate mass value of *m/z* 584.2769 obtained by HRESIMS for the $[M + H]^+$ ion of compound **7** suggested that the compound is likely a trisubstituted spermidine conjugate wherein each spermidine nitrogen atom is incorporated into an amide linkage with a hydroxycinnamic acid type unit. Detailed examination of NMR data revealed the presence of a complex mixture of overlapping signals that could not be readily analyzed. However, the mass and the general appearance of the spectrum were both consistent with a tri-*p*-coumaroylspermidine derivative. The complexity of the spectrum was attributed to the presence of a mixture of conformers presumably due to the presence of a tertiary amide unit and was consistent with literature reports (*10, 12, 18*). NMR data were collected at

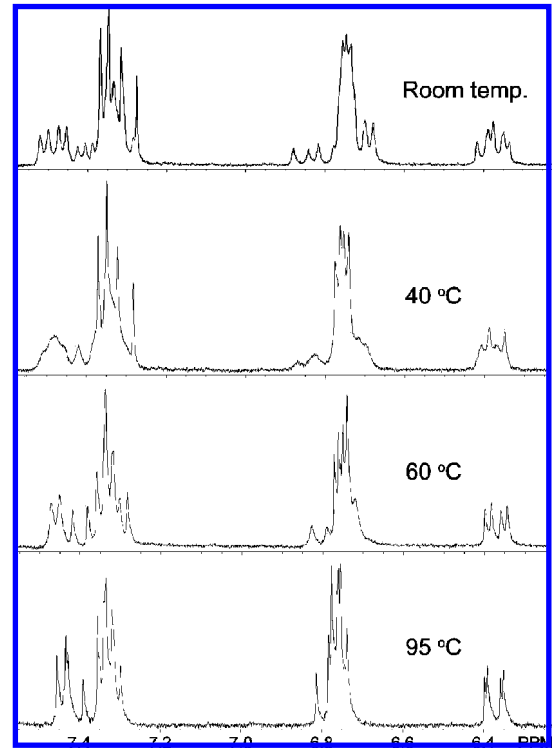

Figure 7. Aromatic/olefinic region of the ^{1}H NMR spectrum of N^1,N^5,N^{10}-tri-*p*-(*EEE*)-coumaroylspermidine **7** showing signal coalescence at elevated temperature (DMSO-d_6).

elevated temperature in an effort to accelerate interconversion of the conformers, thereby simplifying the NMR data. As anticipated, coalescence of signals was observed upon increasing the temperature of a sample dissolved in DMSO-d_6 (**Figure 7**). At 95 °C, a single set of sharp signals was observed, enabling more straightforward interpretation of the data. Clear observation of individual doublets corresponding to the upfield olefinic protons of the *p*-coumaroyl units in this spectrum enabled observation of a 16 Hz *J* value for each signal, resulting in assignment of the *E* geometry for all three olefin units.

The ESI mass spectrum of **6** (**Figure 3**) revealed a molecular mass of 477 Da, and MS^2 data showed a loss of 43 Da from the major daughter ion at *m/z* 358. These results suggested the replacement of one of the *p*-coumaroyl groups found in **7** with an acetyl group in **6**. The ^{1}H NMR data were similar to those of **7**, again showing a complex mixture of signals expected for a mixture of conformers, but were somewhat simpler and also contained a broad singlet characteristic of the acetyl unit of the conformers. As was the case for **7**, ^{1}H NMR analysis at elevated temperature afforded a simplified spectrum that was fully consistent with assignment of **6** as a di-*p*-(*EE*)-coumaroylacetylspermidine. However, the question of regiochemistry is a challenging one. The relative positions of the *p*-coumaroyl and acetyl moieties in **6** could not be deduced from NMR data due to overlap of the methylene signals that occurs even at high field. Similarly, positional isomers of other triacylated spermidine derivatives (coumaroyldicaffeoylspermidine and dicoumaroylcaffeoylspermidine) could not be distinguished on the basis of NMR data (*12*). In the ^{1}H NMR spectrum of **7** (at elevated temperature), it was noted that two of the olefinic signals corresponding to the 8-positions of two of the *p*-coumaroyl units were significantly upfield of the other (δ 6.37 and 6.38 vs 6.80). Given the close similarity in the environments of the two terminal *p*-coumaroyl units (at N-1 and N-10), the most downfield signal of the three was presumed to arise from the

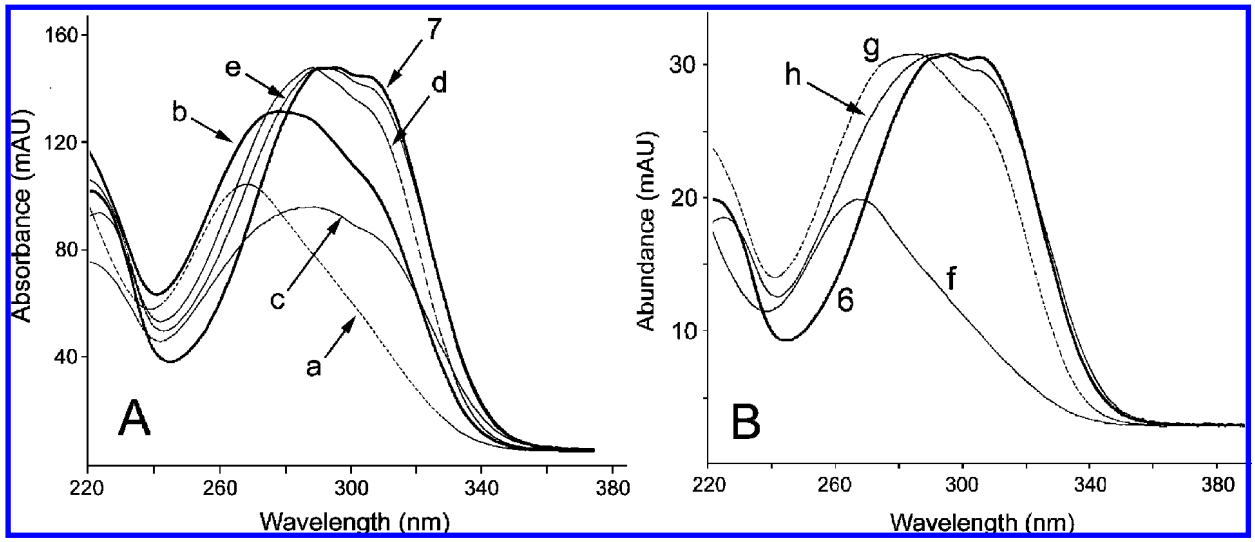

Figure 8. (**A**) UV spectra of N^1,N^5,N^{10}-tri-*p*-(*EEE*)-coumaroylspermidine **7** and its photoisomers. Peaks: a, N^1,N^5,N^{10}-tri-*p*-(*ZZZ*)-coumaroylspermidine; b, mixture of *ZZE* isomers of N^1,N^5,N^{10}-tri-*p*-coumaroylspermidine; c and d, mixture of *ZZE*/*EEZ*isomers; and e, mixture of *EEZ* isomers. (**B**) UV spectra of N^1-acetyl-N^5,N^{10}-di-*p*-(*EE*)-coumaroylspermidine **6** and its photoisomers. Peaks: f, N^1-acetyl-N^5,N^{10}-di-*p*-(*ZZ*)-coumaroylspermidine; g and h, mixture of *ZE* and *EZ* isomers.

corresponding proton in the central *p*-coumaroyl unit (the one at N-5). In the ^{1}H NMR data for **6**, also at elevated temperature, the two *p*-coumaroyl position-8 doublets appeared at δ 6.80 and 6.38, suggesting that one of the terminal *p*-coumaroyl units was missing and thereby suggesting the placement of the acetyl group at a terminus (N-1 or N-10). Even if this conclusion is correct, no decision could be made on the basis of the available NMR data regarding whether the acetyl group was at the N-1 or N-10 position. Evaluation of the EIMS fragmentation pattern for **6** was considered in an effort to locate the acetyl unit, although literature reports indicate that transamidation may lead to ambiguous conclusions. For example, Bokern (*12*), Bigler (*39*), and Hu (*40*) noted the occurrence of a transamidation (the *Zip* reaction) of the $[M + H]^+$ ions for dicoumaroylspermidine under MS conditions. Even so, the EIMS fragmentation pattern enabled a proposal for the location. The base peak in the spectrum (*m*/*z* 147) corresponded to the *p*-coumaroyl acylium ion. The next most abundant peak (*m*/*z* 129) suggested that the acetyl group is located at the N-1 position. Given the corresponding substitution pattern, such an ion could be rationalized by α-cleavage to the N-5 position (between C6 and C7 of the spermidine unit), accompanied by elimination of the N-5 coumaroyl unit. Neither of the other two regioisomers would be expected to give such an ion in a straightforward way. The ion corresponding to the analogous process beginning with α-cleavage on the opposite side of N-5 (*m*/*z* 247) was also observed at moderate intensity. HREIMS data were fully consistent with the expected elemental compositions for all of these key fragments. The EI mass spectrum of triacetylspermidine shows the analogous fragmentations as the two most abundant peaks in the spectrum (*m*/*z* 129 and 143) (*41*). On the basis of these considerations and the fact that the suggestions provided by the NMR and MS data are consistent with each other, the acetyl group of **6** is proposed to be at the N-1 position. However, it was ultimately felt that the data described here do not permit a truly conclusive assignment.

The structure of **5** was deduced from UV and MS data, which matched those previously published (*10*), although the structure assignment in this instance was not considered unambiguous due to insufficient quantities available for analysis by NMR.

Dynamics of Photoisomerization. Interestingly, spermidine conjugates **6** and **7** exhibited very high sensitivity to sunlight. The sample composition (as judged by HPLC profile) changed dramatically and rapidly upon exposure to sunlight for only a very short time. Similar changes were observed upon irradiation with UV light but required longer reaction times. Because sunlight is clearly a natural environmental factor for the peanut plant, efforts to explore this phenomenon were undertaken.

Samples were irradiated with ambient sunlight or UV light, resulting in photoisomerization of the olefin units from the *E* to *Z* forms. Such a transformation is not unexpected for such compounds based on literature precedents (*10, 18, 42*), but the facility and the extent of the conversion were somewhat unexpected. Because of the asymmetry of N^1,N^5,N^{10}-tri-*p*-coumaroylspermidine **7** molecule [$-(CH_2)_3-$ between $N^1$and N^5] and [$-(CH_2)_4-$ between $N^5$and N^{10}], eight stereoisomers having various geometries of the three existing olefinic double bonds are possible as follows: *EEE*, *EEZ*, *EZE*, *EZZ*, *ZEE*, *ZZE*, *ZEZ*, and *ZZZ*. Six chromatographic peaks, including those corresponding to the *EEE* isomer originally present, were observed after only very brief exposure to light (**Figure 5**, 1 min; **Figure 8A**). After longer exposure, the peak for the original *EEE* isomer disappeared and the system came to an equilibrium that was observed in the chromatogram as two major and three minor peaks (**Figure 5**, 1−10 min). LC-MS data indicated that all of the peaks retained the same molecular weight, as expected for a mixture of isomerization products. Samples corresponding to the two major product peaks (peaks a and b, **Figure 5**) were collected by HPLC and analyzed by ^{1}H NMR. Both samples showed the same kind of signal complexity associated with the conformational mixtures observed at room temperature. However, the data for the major component were sufficiently resolved to enable a determination that the olefin *J* values had all changed to 13 Hz, indicating that all of the olefins in this product now bear the *Z* configuration. The greater complexity of the NMR data for the other major peak was presumed to be due to the presence of a mixture of isomers that included two *Z* olefin units and one *E* olefin units, and this was consistent with observations of both 13 and 16 Hz *J* values for individual signals appearing in the olefinic region.

For the dicoumaroylacetylspermidine derivative **6**, only four isomers are possible (*EE*, *EZ*, *ZE*, and *ZZ*). After brief exposure of a sample of pure **6** to sunlight, four peaks, including the original *EE* isomer, were present in the chromatogram (**Figure**

Table 1. Major Constituents of Whole Peanut Flowers (Mean ± SD, μg/g Fresh[a] Tissue; $n = 3$[b])

peanut identity	flower weight (g)	*p*-coumaric acid	quercetin-3-Glc[c] **1**	quercetin-3-GlcUA[c] **2**	isorhamnetin-3-Glc[c] **3**	isorhamnetin-3-GlcUA[c] **4**	DCAS[d] **6**	TCS[e] **7**
				Runner market type				
AT29-1112	179.5	12.5 ± 2.2	66.2 ± 5.1	76.0 ± 4.2	10.1 ± 2.3	13.9 ± 1.8	8.7 ± 1.8	42.3 ± 3.2
G02C	122.6	14.6 ± 1.3	40.7 ± 3.8	89.0 ± 3.5	7.6 ± 1.1	14.8 ± 1.5	6.8 ± 1.1	37.6 ± 2.0
AT3-1114	104.8	15.1 ± 1.8	38.5 ± 1.9	78.1 ± 4.1	13.8 ± 1.5	12.6 ± 1.2	10.1 ± 1.6	59.6 ± 2.5
C724-19-15	90.5	22.0 ± 2.1	44.5 ± 3.5	83.6 ± 3.8	9.9 ± 0.8	18.3 ± 2.1	8.4 ± 0.8	46.0 ± 1.9
Tifrunner	139.6	23.1 ± 2.4	31.5 ± 2.9	58.1 ± 4.3	11.4 ± 1.0	18.8 ± 2.0	10.6 ± 1.2	56.1 ± 2.4
				Virginia market type				
AT3081 R	132.8	6.9 ± 0.7	44.6 ± 3.0	41.2 ± 3.3	6.8 ± 1.4	10.6 ± 1.4	9.2 ± 1.3	44.4 ± 2.7
exp. line A	221.9	8.5 ± 0.9	51.6 ± 3.7	47.2 ± 3.9	8.6 ± 1.8	12.4 ± 2.1	9.2 ± 1.4	42.1 ± 1.8
VC-2	158.7	9.3 ± 1.6	42.3 ± 2.6	85.7 ± 4.1	13.6 ± 2.2	12.4 ± 2.5	7.8 ± 1.2	41.0 ± 2.8
AT3085 RO	162.8	12.2 ± 1.8	44.5 ± 3.1	52.6 ± 3.4	11.1 ± 1.2	12.0 ± 2.0	10.9 ± 2.1	48.8 ± 2.4
Gregory	108.2	13.6 ± 1.8	42.9 ± 3.2	84.1 ± 3.6	7.5 ± 0.7	13.6 ± 1.7	9.5 ± 0.9	51.2 ± 2.2
exp. line B	180.2	16.9 ± 2.5	39.2 ± 2.4	87.9 ± 4.6	8.5 ± 1.4	15.1 ± 2.6	6.7 ± 1.0	35.5 ± 3.0

[a] A multiplication factor of 9.3 should be used for recalculation of the major constituents' content in dry weight of plant material. [b] Three subsamples from each sample that represents a peanut line were analyzed. [c] GlcUA, glucuronyl unit; Glc, glucosyl unit; [d] DCAS, N^1-acetyl-N^5,N^{10}-di-*p*-(*EE*)-coumaroylspermidine **6**. [e] TCS, N^1,N^5,N^{10}-tri-*p*-(*EEE*)-coumaroylspermidine **7**.

4, 20 s; **Figure 8B**). However, by the end of a 90 s exposure, only two major and one minor peaks were detected, and the original *EE* isomer was absent (**Figure 4**, 90 s). Continued irradiation for 15 min did not cause further change in the composition or ratio of the components of the mixture (**Figure 4**, 15 min).

Separation of the photoisomers could be achieved on a C_{18} stationary phase only when CH_3CN was used as an organic modifier of the mobile phase. Isocratic elution was found to be superior to gradient elution and allowed for baseline separations of the isomers. The ratios of isomers obtained in the products at equilibrium were judged to be reflective of approximately a 6:1 preference for *Z* over *E* at each possible olefin position, which is reasonably consistent with expectations based on literature precedents for photoisomerization of similar compounds (*10, 42*). Analogous results were obtained regardless of temperature, as the same chromatographic results were obtained over similar time periods when the experiments were conducted at −95, 30, and 100 °C. Variation in the solvent employed (MeOH or $CH_3CN-H_2O-HCOOH$) also led to no change in the results.

Production of Major Secondary Metabolites. Because of a lack of the data in literature on peanut flower constituents, the major low molecular weight secondary metabolites in the whole flower extracts were investigated first. HPLC chromatograms of these extracts revealed the presence of three major components (1, 2, and 7; **Figure 6**). Extracts of individual peanut flower organs (**Figure 2**) contained diverse major compounds. The standard and wings contained high concentrations of **1**, **2**, **3**, and **4** (**Figure 6**). The wings tended to accumulate **1** and **2** at a lower ratio to **3** and **4** than the standard. Flavonoid conjugates **1**–**4** were virtually the only metabolites that were extracted with MeOH. These compounds are commonly found in other plants (*7, 37*), but **1**−**4** are reported in peanut flowers for the first time in the present study. On the contrary, flavonoids **1**−**4** were not detected in the keel, which was instead found to accumulate spermidine conjugates **5**−**7**. The latter compound was found in high concentrations (**Table 1**). Quantitation of **5** in the whole flower extracts could not be accomplished due to its low concentrations. The hypanthium extract was comprised mainly of phenolic acids, of which *p*-coumaric acid is most notable given its involvement in the formation of spermidine conjugates **5**−**7**. Concentrations of *p*-coumaric acid in whole flowers are reflected in **Table 1**.

Although there was a significant difference in flower weight among some lines (**Table 1**), there was no correlation between the weight (and indirectly the number of flowers) and the flavonoid and spermidine conjugate production (**Table 1**). Side-by-side comparison of production of the same compounds by the two market type peanut varieties represented in **Table 1** did not reveal any significant difference. Production of flavonoids and spermidines was uniform, but there was a significant difference between some individual lines of both market types. For example, production of *p*-coumaric acid by Tifrunner was the highest of all tested lines. At the same time, the overall concentration of the flavonoid conjugates **1**−**4** was the lowest in this line, and there was a significant difference between the production of **1** and **2** by Tifrunner and other representatives of the runner type peanuts. In some lines, only two metabolites (**2** and *p*-coumaric acid) varied significantly in Virginia market type peanuts; Gregory and experimental line B accumulated these metabolites in about twice the concentration as compared with AT3081 R and experimental line A. At the same time, concentrations of **7** did not vary significantly among all tested lines. It seems that the biosynthesis of **7** by the flower reproductive organs is a well-regulated process that does not depend on peanut genotypes (**Table 1**).

In the present study, compounds **6** and **7** demonstrated very high sensitivity to sunlight (**Figures 6** and **7**). It should be emphasized that only *E* isomers of the spermidine conjugates **5**−**7** were detected in peanut flowers when extracts and solutions were protected from light. The configurational *E*/*Z* isomeric mixtures were found only during isolation of the products and in other experiments when protection from light was not assured. It should also be noted that coumaroylacetylspermidine **6** is not an artifact since it was detected in high concentrations under all extraction conditions, including soaking fresh whole flowers in MeOH at 4 °C.

Earlier experiments (*33*) demonstrated that in strawberry, a short-day plant, spermidine conjugates along with other free and bound polyamines were accumulated in the shoot tips during floral induction and before floral emergence. In vegetative shoot tips from plants grown continuously during long days, conjugated spermidines as well as free and bound amines did not appear; free and bound polyamine concentrations were low, and no change was observed. Male sterile flowers were distinguished by their lack of conjugated spermidines and free and bound amines. Apparently, light directly or indirectly regulates conjugated spermidine production/accumulation, but the mechanism of this phenomenon is unknown.

The peanut flower reproductive organs are located in a curved keel (**Figure 2**) that is formed by two petals fused along the

dorsal edges to the apex but open ventrally at the base (*1*). The keel seems to be well-protected by the petals from the UV portion of the sunlight taking into account the high concentrations of the flavonoids and the presence of carotenoids. However, dormant flowers may be exposed to sunlight for several hours during daytime, and in this unlikely scenario, the chemical shield may not necessarily be able to completely block the radiation that may be absorbed by the spermidines. If so, the formation of the spermidine photoisomers (**Figures 6** and **7**) is possible, considering the extremely high photosensitivity of the major spermidine conjugates **7** (**Figure 5**) and **6** (**Figure 4**). However, it is also possible that the flower reproductive organs may have some way to maintain spermidines **5**–**7** in their natural *E* configuration. In the present study, the photoisomers were not detected, as the flowers were collected at sunrise, at the time when fertilization occurs. Additional experiments with dormant flowers may reveal the presence or absence of the photoisomers. Whether photoisomerization may take place in peanut flowers in the daytime and whether the photoisomers may play a role in one or more biochemical processes regulating plant reproduction are questions that remain to be addressed.

The present study revealed the production of flavonoid (**1**–**4**) and spermidine conjugates (**6** and **7**) in the peanut flower at high levels. All major metabolites have been reported in the flowers for the first time. One of the metabolites, N^1-acetyl-N^5,N^{10}-di-*p*-(*EE*)-coumaroylspermidine **6**, has not been previously reported in plants. Study of the changes that occur in **6** and **7** upon irradiation with sunlight revealed the formation of several intermediate photoisomers. Both flavonoid and spermidine conjugates may play a protective role against pests as reflected in the cited literature. The exact role of **6** is unknown, but as has been suggested for **7**, the compound may be involved in regulating the plant reproductive process.

ABBREVIATIONS USED

ESI, electrospray ionization; HRESIMS, high-resolution electrospray ionization mass spectrometry; EIMS, electron impact mass spectrometry; HREIMS, high-resolution electron impact mass spectrometry; HMBC, heteronuclear multiple bond correlation; HMQC, heteronuclear multiple quantum correlation.

ACKNOWLEDGMENT

We thank Dr. C. Chen for providing fresh peanut flowers and his comments and B. Tennille for collecting the flowers. Support for the Iowa group from the National Science Foundation (CHE-0718315) is gratefully acknowledged.

Supporting Information Available: UV spectra (in mobile phase #1) of peanut flower flavonoid conjugates. This material is available free of charge via the Internet at http://pubs.acs.org.

LITERATURE CITED

(1) Smith, B. W. *Arachis hypogaea*. Aerial flower and subterranean fruit. *Am. J. Bot.* **1950**, *37*, 802–815.
(2) Oakes, A. J. Pollen behavior in the peanut (*Arachis hypogaea* L.). *Agron. J.* **1958**, *50*, 387.
(3) Sprenkel, R. K. Identification and monitoring of insect pests in peanut. http://edis.ifas.ufl.edu/IN176 (accessed 02/07/2008).
(4) Smith, J. W.; Barfield, C. Management of preharvest insects. In *Peanut Science and Technology*; Pattee, H. E., Young, G. T., Eds.; American Peanut Research and Education Society, Inc.: Yoakum, TX, 1982; 825 pp.
(5) Insect and mite control in field crops 2007—Readers' note. http://www.dpi.nsw.gov.au/_data/assets/pdf_file/0008/173690/insect-mite-control-crops-pt4.pdf (accessed 02/07/2008).
(6) Harborne, J. B.; Grayer, R. J. Flavonoids and insects. In *The Flavonoids: Advances in Research Since 1986*; Harborne, J. B., Ed.; Chapman and Hall: London, United Kingdom, 1993; 676 pp.
(7) Hermann, K. Flavonols and flavones in food plants: A review. *J. Food Technol.* **1976**, *11*, 433–442.
(8) Havsteen, B. H. The biochemistry and medical significance of the flavonoids. *Pharmacol. Ther.* **2002**, *96*, 67–202.
(9) Martin-Tanguy, J.; Cabanne, F.; Perdrizet, E.; Martin, C. The distribution of hydroxycinnamic acid amides in flowering plants. *Phytochemistry* **1978**, *17*, 1927–1928.
(10) Werner, C.; Hu, W.; Lorenzi-Riatsch, A.; Hesse, M. Di-coumaroylspermidines and tri-coumaroylspermidines in anthers of different species of the genus *Aphelandra*. *Phytochemistry* **1995**, *40*, 461–465.
(11) Nimtz, M.; Bokern, M.; Meurer-Grimes, B. Minor hydroxycinnamic acid spermidines from pollen of *Quercus dentate*. *Phytochemistry* **1996**, *43*, 487–489.
(12) Bokern, M.; Witte, L.; Wray, V.; Nimtz, M.; Meurer-Grimes, B. Trisubstituted hydroxycinnamic acid spermidines from *Quercus dentata* pollen. *Phytochemistry* **1995**, *39*, 1371–1375.
(13) Zamble, A.; Sahpaz, S.; Hennebelle, T.; Carato, P.; Bailleul, F. N^1,N^5,N^{10}-Tris(4-hydroxycinnamoyl)spermidines from *Microdesmis keayana* roots. *Chem. Biodiversity* **2006**, *3*, 982–989.
(14) Strack, D.; Eilert, U.; Wray, V.; Wolff, J.; Jaggy, H. Tricoumaroylspermidine in flowers of Rosaceae. *Phytochemistry* **1990**, *29*, 2893–2896.
(15) Meurer, B.; Wray, V.; Grotjahn, L.; Wiermann, R.; Strack, D. Hydroxycinnamic acid spermidine amides from pollen of *Corylus avellana* L. *Phytochemistry* **1986**, *25*, 433–435.
(16) Meurer, B.; Wiermann, R.; Strack, D. Phenylpropanoid patterns in Fagales pollen and their phylogenetic relevance. *Phytochemistry* **1988**, *27*, 823–828.
(17) Perez-Amador, M. A.; Carbonell, J.; Navarro, J. L.; Moritz, T.; Beale, M. H.; Lewis, M. J.; Hedden, P. N^4-Hexanoylspermidine, a new polyamine-related compound that accumulates during ovary and petal senescence in pea. *Plant Physiol.* **1996**, *110*, 1177–1186.
(18) Meurer, B.; Wray, V.; Wiermann, R.; Strack, D. Hydroxycinnamic acid-spermidine amides from pollen of *Alnus glutinosa*, *Betula verrucosa* and *Pterocarya fraxinifolia*. *Phytochemistry* **1988**, *27*, 839–843.
(19) Youhnovski, N.; Filipov, S.; Linden, A.; Guggisberg, A.; Werner, C.; Hesse, M. Two macrocyclic spermine alkaloids from *Aphelandra fuscopunctata* (Acanthaceae). *Phytochemistry* **1999**, *52*, 1717–1723.
(20) Martin, C.; Kunesch, G.; Martin-Tanguy, J.; Negrel, J.; Paynot, M.; Carré, M. Effect of cinnamoyl putrescines on in vitro cell multiplication and differentiation of tobacco explants. *Plant Cell Rep.* **1985**, *4*, 158–160.
(21) Smith, T. A.; Best, G. R. Distribution of the hordatines in barley. *Phytochemistry* **1978**, *17*, 1093–1098.
(22) Nomura, T.; Sue, M.; Horikoshi, R.; Tebayashi, S.; Ishihara, A.; Endo, T. R.; Iwamura, H. Occurrence of hordatines, the barley antifungal compounds, in a wheat-barley chromosome addition line. *Genes Genet. Syst.* **1999**, *74*, 99–103.
(23) Guillet, G.; De Luca, V. Wound-inducible biosynthesis of phytoalexin hydroxycinnamic acid amides of tyramine in tryptophan and tyrosine decarboxylase transgenic tobacco lines. *Plant Physiol.* **2005**, *137*, 692–699.
(24) Jin, S.; Yoshida, M.; Nakajima, T.; Murai, A. Accumulation of hydroxycinnamic acid amides in winter wheat under snow. *Biosci., Biotechnol., Biochem.* **2003**, *67*, 1245–1249.
(25) Facchini, P. J.; Hagel, J.; Zulak, K. G. Hydroxycinnamic acid amide metabolism: physiology and biochemistry. *Can. J. Bot.* **2002**, *80*, 577–589.
(26) Walters, D.; Meurer-Grimes, B.; Rivora, I. Antifungal activity of three spermidine conjugates. *FEMS Microbiol. Lett.* **2001**, *201*, 255–258.
(27) Klose, M. K.; Atkinson, J. K.; Mercier, A. J. Effects of a hydroxycinnamoyl conjugate of spermidine on arthropod neuromuscular junctions. *J. Comp. Physiol. A* **2002**, *187*, 945–952.

(28) Lin, S.; Mullin, C. A. Lipid, polyamide, and flavonol phagostimulants for adult western corn rootworm from sunflower (*Helianthus annuus* L.) pollen. *J. Agric. Food Chem.* **1999**, *47*, 1223–1229.
(29) Cabanne, F.; Dalebroux, M. A.; Martin-Tanguy, J.; Martin, C. Hydroxycinnamic acid amides and ripening to flower of *Nicotiana tabacum* var *xanthi* n.c. *Physiol. Plant* **1981**, *53*, 399–404.
(30) Martin-Tanguy, J.; Perdrizet, E.; Prevost, J.; Martin, C. Hydroxycinnamic acid amides in fertile and cytoplasmic male sterile lines of maize. *Phytochemistry* **1982**, *21*, 1939–1945.
(31) Ponchet, M.; Martin-Tanguy, J.; Marais, A.; Martin, C. Hydroxycinnamoyl acid amides and aromatic amines in the inflorescences of some araceae species. *Phytochemistry* **1980**, *21*, 2865–2869.
(32) Martin-Tanguy, J. Conjugated polyamines and reproductive development: Biochemical, molecular and physiological approaches. *Physiol. Plant* **1997**, *100*, 675–688.
(33) Tarenghi, E.; Martin-Tanguy, J. Polyamines, floral induction and floral development of strawberry (*Fragaria ananassa* Duch.). *Plant Growth Regul.* **1995**, *17*, 157–165.
(34) Ma, C.-M.; Nakamura, N.; Hattori, M. Inhibitory effects on HIV-1 protease of tri-*p*-coumaroylspermidine from *Artemisia caruifolia* and related amides. *Chem. Pharm. Bull.* **2001**, *49*, 915–917.
(35) Funatogawa, K.; Hayashi, S.; Shimomura, H.; Yoshida, T.; Hatano, T.; Ito, H.; Hirai, Y. Antibacterial activity of hydrolyzable tannins derived from medicinal plants against *Helicobacter pylori*. *Microbiol. Immunol.* **2004**, *48*, 251–261.
(36) Mullen, W.; Boitier, A.; Stewart, A. J.; Crozier, A. Flavonoid metabolites in human plasma and urine after the consumption of red onions: Analysis by liquid chromatography with photodiode array and full scan tandem mass spectrometric detection. *J. Chromatogr. A* **2004**, *1058*, 163–168.
(37) Schieber, A.; Keller, P.; Streker, P.; Klaiber, I.; Carle, R. Detection of isorhamnetin glycosides in extracts of apples (*Malus domestica* cv. "Brettacher") by HPLC-PDA and HPLC-APCI-MS/MS. *Phytochem. Anal.* **2002**, *13*, 87–94.
(38) Boumaza, O.; Mekkiou, R.; Seghiri, R.; Sarri, D.; Benayache, S.; Garcia, V. P.; Bermejo, J.; Benayache, F. Flavonoids and isoflavonoids from *Genista tricuspidata*. *Chem. Nat. Compd.* **2006**, *42*, 730–731.
(39) Bigler, L.; Schnider, C. F.; Hu, W.; Hesse, M. Electrospray-ionization mass spectrometry. Part 3. Acid-catalyzed isomerization of N,N′-bis[(E)-3-(4-hydroxyphenyl)prop-2-enoyl]spermidines by the Zip reaction. *Helv. Chim. Acta* **1996**, *79*, 2152–2163.
(40) Hu, W.; Reder, E.; Hesse, M. Electrospray-ionization mass spectrometry. Part 2. Neighboring-group participation in the mass-spectral decomposition of 4-hydroxycinnamoyl-spermidines. *Helv. Chim. Acta* **1996**, *79*, 2137–2151.
(41) *The Wiley Registry of Mass Spectral Data*, 7th ed.; John Wiley and Sons: New York, 2000.
(42) Lewis, F. D.; Elbert, J. E.; Upthagrove, A. L.; Hale, P. D. Structure and photoisomerization of (*E*)- and (*Z*)-cinnamamides and their lewis acid complexes. *J. Org. Chem.* **1991**, *56*, 553–561.

Received for review December 15, 2007. Revised manuscript received February 15, 2008. Accepted February 20, 2008.

JF703652A